

POLE-PLACEMENT CONTROL OF A WALL CLIMBING VORTEX MACHINE

TARIQ P. SATTAR, MALTE LORBACH, SALMAN HUSSAIN,
HERNANDO LEON RODRIGUEZ

*Centre for Automated and Robotic NDT, Faculty of Engineering, Science & the Built
Environment, London South Bank University, 103 Borough Road, London SE1 0AA*

The paper presents the performance of a control system designed to maintain a desired negative pressure to support the payload of a wall climbing robot with a Vortex machine on different climbing surfaces. The control objective is to provide fast response to changes in pressure demands and air leakage when a vacuum chamber is dragged over different climbing surfaces by a wheeled robot. Experiments have been performed on a single vacuum chamber in which a negative pressure is created by a very cheap AC motor and control is applied by changing the speed of the motor. A pole-placement control system is shown to decrease the time constant of the Vortex system from an open-loop value of 2.85 second to a closed-loop value of 0.15 second.

1. Introduction

An active negative pressure system combined with a wheeled robot seems to be the best solution for climbing rapidly on non-ferrous surfaces [1, 2].

An experimental setup to study the problem of controlling an active negative pressure system is shown in figure 1. A very cheap 240VAC motor from a domestic vacuum cleaner is speed controlled by using a phase controlled power regulator. A control signal from a PC via a DAC changes the phase on the power regulator. A single negative pressure chamber is created by using an air inflated rubber tube from a small tyre as a seal. A membrane constructed from a nylon material with very low coefficient of friction contains the rubber tube and allows the machine to slide on a climbing surface while the rubber tube provides the surface adaptability to cope with uneven surfaces. The area of the circular chamber is 0.02m^2 and volume is 0.002m^3 .

We call this device a Vortex machine loosely on the assumption that the motor and extractor fan create an air vortex which creates a negative pressure in the chamber between the machine and the climbing surface. A gage pressure sensor with an output voltage range $V_{\text{out}} = 0$ to -10V is used to measure the negative pressure. The pressure conversion is $P = V_{\text{out}} \times 931.82 + (\text{atmospheric pressure})$, Pa. This setup promises to give the fastest reaction to pressure

changes in the chamber due to air leakages as the robot moves over cracks and surface irregularities. If the robot travels over different surfaces e.g. makes a transition from a concrete surface to a brick surface, then the dynamics of the Vortex machine changes and it becomes necessary to adapt the control system to the new dynamics. Controlling the speed of the machine also gives an opportunity to vary the adhesion forces for different purposes. For example, during motion the adhesion forces could be reduced to a predetermined threshold to reduce friction forces. When stationary, the force could be increased to maximum to provide a more stable platform for tasks such as arm manipulation or inspection sensor deployment. A further advantage is that energy savings can be made as the control system will slow down the motor when the surface is smooth and the desired pressure to support a given payload is obtained with lower control voltages. This will be important for autonomous robots when an on-board battery supplies the power.

Experiments show that the Vortex system has a very low margin of stability and that PID type of controllers may not be suitable to obtain fast changes of pressure to adapt to unexpected air leakages due to surface changes and irregularities. A pole-placement controller can obtain faster responses that are suitable for climbing robots.

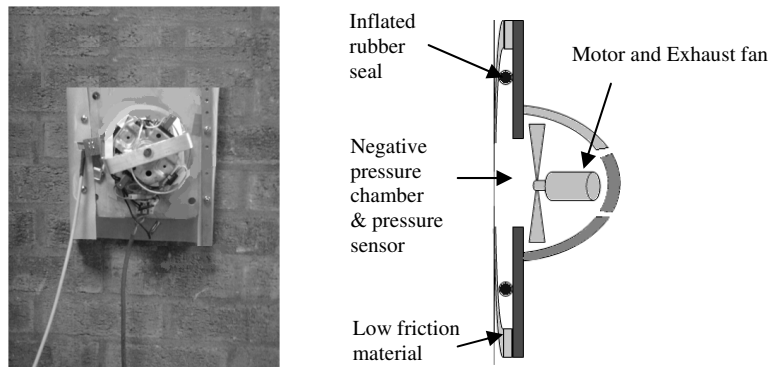


Figure 1: The experimental Vortex machine adhering to a brick wall and schematic

2. The Model of the Vortex Machine

The pressure dynamics inside the chamber can be modeled by applying simplified fluid mechanics (see [3], [4], [5]) but here we have derived an estimated model from measurements on the vortex system operating in a linear region of the system dynamics.

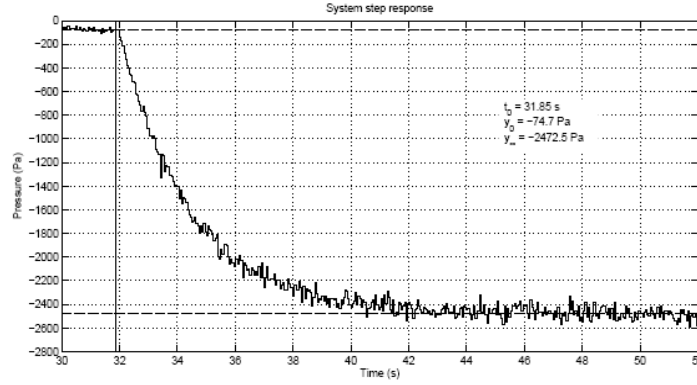


Figure 2: Open-loop step response, input step changed from 2.5V to 3V at $t_0 = 31.85 \text{ s}$, Time constant $\approx 2.85\text{s}$

The dynamics of the Vortex machine are estimated by applying a step voltage change of 0.5V above the dead zone voltage of 2.5V i.e. 3 volts is actually applied but the pressure inside the chamber does not become negative relative to atmospheric pressure till 2.5 V. Figure 2 shows that the negative pressure response $y(t)$ has a time constant of 2.85s, $y(0) = -74.7 \text{ Pa}$ $y(\infty) = -2472.5 \text{ Pa}$.

The first order model that approximates the response in figure 2, feeding back the pressure sensor reading in pascal (Pa), has the transfer function at the operating point of 2.5V:

$$\frac{Y(s)}{U(s)} = \frac{-0.1753}{s + 0.351} \quad \text{Eq (1)}$$

This system has a time constant of 2.85s. The system pole at $s = -0.351$ gives a very small margin of relative stability and attempts to control it with PID controller's results in instability or very slow response to changes in demand.

Figure 3 shows a proportional controller exhibiting stability for low demand values but becoming unstable for larger demands.

The dynamics of the Vortex machine depend on the air leakage into the vacuum chamber and for smooth surfaces this is determined by the effectiveness of the sealing system.

Figure 4 shows the steady-state characteristic of the system with pressure against the applied motor voltage when the Vortex machine is on a smooth steel surface. The two curves are for the cases where (a) a brush skirting is used to create a seal with the surface (b) an inflated rubber tube is used to create a seal. Case (a) provides very little friction during motion of the robot but better

negative pressures and hence adhesion forces are obtained for case (b). Hence we have used this system to create the sealing. For case (b) the system is linear for motor control voltages between approximately 3V and 6V. Therefore, the usable pressure range is approximately -3030Pa (-3.25V) and -7900Pa (-8.5V) relative to standard air pressure.

Figure 5 shows the steady state values of Vortex chamber pressure on different types of climbing surface for various values of voltage applied to the motor power controller. The effective operating voltage in all cases is 2.5V with the pressure sensor reaching its maximum output of -10 V with an input of 4 V. The range of control input that can be applied to the motor power controller is 0-10V but figure 5 suggests that on level surfaces this may not be needed but will be in reserve for unexpected leakages.

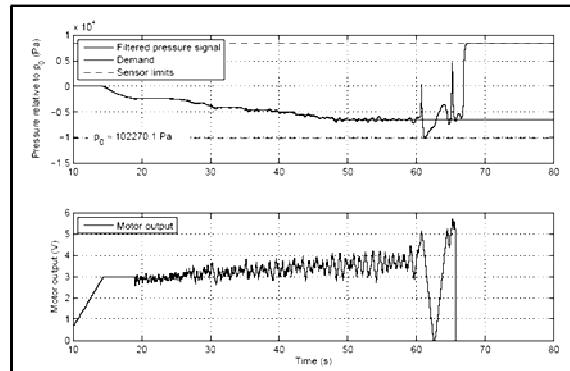


Figure 3: PID control of Vortex machine showing unstable behaviour for larger pressure demands.

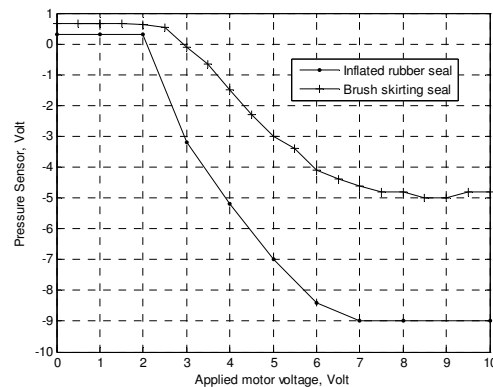


Figure 4: Steady state pressure in the Vortex chamber versus Motor voltage. Steel surface.

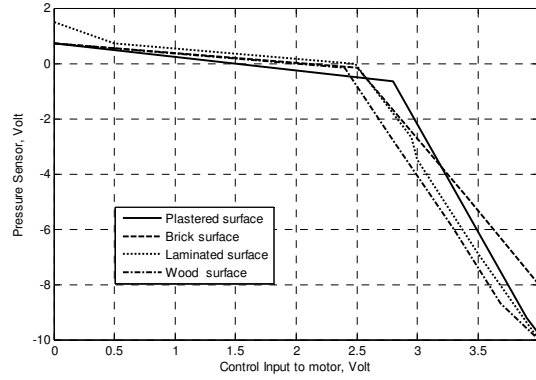


Figure 5: Steady state pressure in Vortex chamber against motor voltage on different types of surface

The model that approximates the transient response between the input control to the motor and the negative pressure in the Vortex chamber (measured in sensor voltage) is as follows:

$$\frac{Y(s)}{U(s)} = G_p(s) = \frac{-1.807}{s + 0.351} \quad Eq (2)$$

3. Proportional Control

The system was tested in a closed loop with a unity negative feedback and a proportional controller with gain K . The closed-loop transfer function is:

$$T(s) = \frac{\frac{-1.807K}{s + 0.351}}{1 + \frac{-1.807K}{s + 0.351}} = \frac{-1.807K}{s + (0.351 - 1.807K)}$$

To keep the system stable its pole has to be in the left-hand side of the s -plane $s = -(0.351 - 1.807K)$ For stability $K < 0.1942$ is a necessary condition.

Tests were performed with this proportional controller at various values of gain K . Stable control was obtained with values of $K \leq 0.1$ but it is unable to track changes in demand. The margin of stability is very low due to the closed-loop pole being very close to the boundary of stability and the pressure and the motor control signals oscillate without a change at the input.

Conclusion: PID control is not suitable for this system as stability is only possible for low values of proportional gain which in turn does not provide sufficient power to rapidly track changing demands.

4. Digital Control: Pole-Placement Control

To overcome this problem a digital pole-placement controller was tested and found to be capable of ensuring stability and a fast tracking capability. The z-transfer function of the Vortex machine (using the model in equation 2), with zero-order hold and sampling period of $T = 0.05\text{s}$ (i.e. 20Hz frequency).

$$\frac{Y(z)}{U(z)} = G_p(z) = \frac{-0.08956}{z - 0.9826}$$

$$G_p(z^{-1}) = \frac{-0.08956z^{-1}}{1 - 0.9826z^{-1}} \quad Eq(3)$$

The system pole at $z = 0.9826$ lies very close to the stability boundary at $z = 1$, hence the susceptibility of the system to become unstable with larger input changes and noise.

4.1. Pole-placement control

Expressing the system as a DARMA difference equation model:

$$\frac{y(k)}{u(k)} = \frac{z^{-d}B(z^{-1})}{A(z^{-1})} \quad Eq(4)$$

$$\text{Control Law: } u(k) = \frac{-G(z^{-1})}{F(z^{-1})} y(k) + \frac{H(z^{-1})}{F(z^{-1})} r(k) \quad Eq(5)$$

Then the closed-loop equation is obtained by substituting equation 5 into 4.

$$y(k) = \frac{-z^{-d}B(z^{-1})G(z^{-1})}{A(z^{-1})F(z^{-1})} y(k) + \frac{z^{-d}B(z^{-1})H(z^{-1})}{A(z^{-1})F(z^{-1})} r(k)$$

$$(A(z^{-1})F(z^{-1}) + z^{-d}B(z^{-1})G(z^{-1}))y(k) = z^{-d}B(z^{-1})H(z^{-1})r(k)$$

Solve the Diophantine equation to place desired poles given by the polynomial $P(z^{-1})$:

$$A(z^{-1})F(z^{-1}) + z^{-d}B(z^{-1})G(z^{-1}) = P(z^{-1}) \quad Eq(6)$$

The closed-loop equation becomes $y(k) = \frac{z^{-d}B(z^{-1})H(z^{-1})}{P(z^{-1})} r(k)$ and the poles are placed at the desired positions. The steady state error is reduced to zero by selecting $H(z^{-1}) = \frac{P(1)}{B(1)}$

We have designed a pole-placement servo controller to place a closed-loop pole at $z = 0.9$ with polynomial $P(z^{-1}) = 1 - 0.9 z^{-1}$. This will not make the system response much faster than the open-loop case but will shift the pole away from the stability boundary at $z = 1$.

Control Parameters: $G = -0.922286$, $F = 1$, $H = -1.11656$

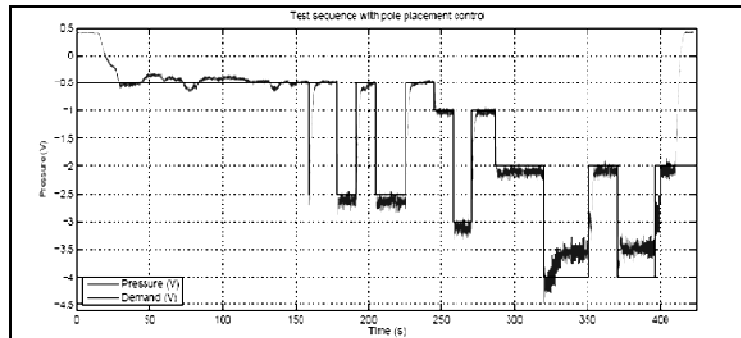


Figure 6: Pressure demand followed with Pole-placement controller placing a pole at $z = 0.9$

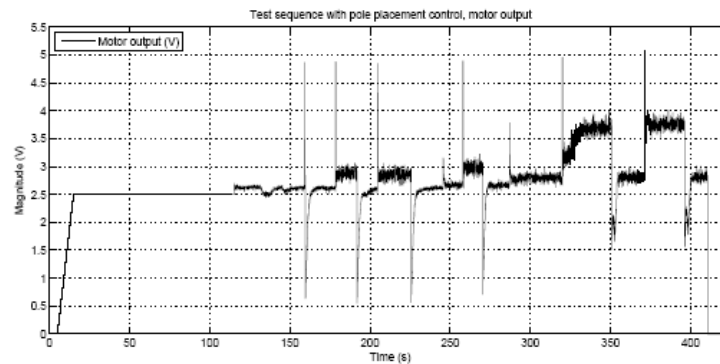


Figure 7: Control signal applied by the Pole-placement controller

The system response with this controller is shown in figure 6 and the control effort in figure 7. Due to the static characteristic, which is not entirely linear, a steady state error remains at higher demands. However, the system is able to react quickly to demand changes. The time constant is approximately $T = 0.35s$.

Faster response can be obtained by placing poles towards the origin of the z -plane. Figures 8 and 9 show results obtained by placing poles at $z = 0.5$ as well as at $z = 0.9$. The operating point in controller implementation is at control input of 3.5V to overcome the system dead-zone. The control signal range is 0-10V.

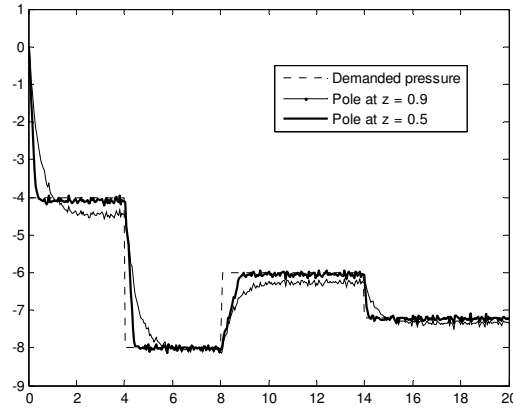


Figure 8: Pressure control in the Vortex chamber placing poles at $z = 0.9$ and $z = 0.5$

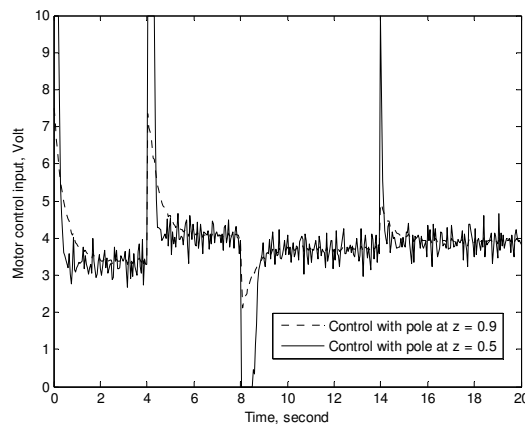


Figure 9: Control signal applied to motor controller when pole placed at $z = 0.9$ and $z = 0.5$. Operating voltage is 3.5V and range of control signal is from zero to 10 V.

A fine tuning facility for both the H and G gains around their calculated values is provided to get better transient and tracking of the demand signal. The pole-placement controller placing poles at $z = 0.5$ gives a faster response with time constant of 0.15s and also less steady-state error. This performance is at the expense of larger control effort and hence energy usage.

5. Conclusion

The pole-placement controller is able to stabilize the Vortex system and gives nearly twenty times faster following of demands in pressure change (from a time

constant of 2.85s in open-loop to 0.15s in the closed-loop) when operating on the same surface. The controlled system should enable a climbing robot to adapt rapidly to changes in surface quality as it moves around. The control system has been tested on a number of surfaces ranging from smooth laminated surfaces to brick walls. Future work will test the control system as the robot makes transitions from one type of surface to another.

The Vortex machine controlled here is manufactured for domestic vacuum cleaners. It is very cheap, costing a few Euros, allowing a low cost climbing robot to be built by incorporating many machines in multi-chamber robots to meet larger payload demands, provide robust adhesion when the robot moves over cracks, and ensure robot safety.

References

1. Hillenbrand, C. and Berns, K. (2004), A climbing robot based on under pressure adhesion for the inspection of concrete walls. In 35th International Symposium on Robotics (ISR), page 119, Paris, France.
2. Hillenbrand, C., Schmidt, D., and Berns, K. (2008). Crooms - Development of a Climbing Robot with Negative Pressure Adhesion for Inspections. In *Industrial Robot* Volume 35 Issue 3, Emerald Group Publishing Ltd., May 2008.
3. Zhijian Jiang, Jun Li, Xueshan Gao, Ningjun Fan, and Boyu Wei. Study on pneumatic wall climbing robot adhesion principle and suction control. In *Robotics and Biomimetics, 2008. ROBIO 2008. IEEE International Conference on*, pages 1812–1817, Feb. 2009.
4. Jun Li, Xueshan Gao, Ningjun Fan, Kejie Li, and Zhihong Jiang. Bit climber: A centrifugal impeller-based wall climbing robot. In *Mechatronics and Automation, 2009. ICMA 2009. International Conference on*, pages 4605–4609, Aug. 2009. 3
5. Young Kouk Song, Chang Min Lee, Ig Mo Koo, Duc Trong Tran, Hyungpil Moon, and Hyouk Ryeol Choi. Development of wall climbing robotic system for inspection purpose. In *Intelligent Robots and Systems, 2008. IROS 2008. IEEE/RSJ International Conference on*, pages 1990 –1995, Sep. 2008. 3